

Contents list available at CBIORE journal website

Remarkable Energy Development

Journal homepage: https://ijred.cbiore.id



Research Article

A porous activated carbon derived from banana peel by hydrothermal activation two-step methods

Yusup Hendronursito^{a, b}, Widi Astuti^b, Harsojo Sabarman^a, Iman Santoso^a

Abstract. Activated carbon from biomass is often the best choice for use as an environmentally friendly supercapacitor material. This study aims to identify the effect of hydrothermal (HT) treatment on the structure and specific surface area (SSA) of activated carbon made from banana peels. The carbon was activated through two stages of HT and physical activation without KOH. HT was carried out at a temperature of 200°C with a holding time of 2 or 6 hours. The hydrocarbon was then activated in the second stage using nitrogen gas at a temperature of 700°C for 1 hour with a flow rate of 100 mL/min. In the treatment process without HT, two stages of activation, variations of activators (water, H₃PO₄, and PEG6000), water volume ratio, and holding time were studied. SSA was measured using the Brunauer–Emmett–Teller adsorption method. X-ray crystallography was used to identify the crystal structure and the surface morphology of activated carbon was observed using FE-SEM. The results showed that the activation method and process conditions greatly affected the SSA of activated carbon. HT activation resulted in SSA of 476.9 m²/g. The degree of crystallization of activated carbon enhanced the HT effect. The spherical structure of activated carbon was formed when H₃PO₄ was added, while the layered structure was formed when PEG6000 was used. Overall, the two-step activation preceded by HT process with the addition of H₃PO₄ resulted in activated carbon with better SSA and carbon structure and has the potential to be used in a wide range of applications such as electrode supercapacitors.

Keywords: activated carbon; banana peel; hydrothermal; specific surface area; H₃PO₄; supercapacitor



@ The author(s). Published by CBIORE. This is an open access article under the CC BY-SA license (http://creativecommons.org/licenses/by-sa/4.0/).

Received: 15th Nov 2024; Revised: 10th January 2025; Accepted: 10th Feb 2025; Available online: 23rd Feb 2025

1. Introduction

Hydrothermal Carbonization (HT) is a thermal treatment that occurs in aqueous medium heated at subcritical temperatures under self-generated pressure. The process was performed in a tightly closed container at a temperature of 180-250 °C and a pressure of 2-6 MPa for 5-240 (Lin et al., 2023; Zhang et al., 2018; Zhang et al., 2019). Hydrothermal treatment proposes environmental advantages due to relatively low process temperature and the use of water medium. HT can be applied to biomass containing high water content without requiring drying, making it advantageous compared to other processes that require drying of raw materials as a pre-treatment (Lestari et al., 2022; Nonchana & Pianthong, 2020). Because it works at relatively low temperatures, this method also requires less energy than the pyrolysis carbonization. In addition, the byproducts of HT are gases such as NO2 and SO2 which can dissolve in water media to form salts and acids, making them more environmentally friendly because they do not escape into the atmosphere. However, this method still has weaknesses because the activated carbon product produced has a low specific surface area (SSA).

To increase the SSA value of HT products, pre-treatment and post-treatment processes are usually carried out. The pretreatment carried out includes size refinement, sieving according to the desired size, and soaking in a chemical activator. Meanwhile, the post-treatment carried out is chemical and physical activation using inert gases such as nitrogen or argon which aims to activate carbon products and increase product porosity (MacDermid-Watts *et al.*, 2021). The effect of phosphoric acid on the surface properties of hydrochar made from banana peels has been studied. The addition of 50% H₃PO₄ produces a carbon product with a surface area (SBET) of 28.8 m²/g (Zhou, Chen, Feng, *et al.*, 2017). Poly Ethylene Glycol (PEG) has also been used as a reactant in the HT process which has a better effect on the crystallinity of the product which is characterized as strong and sharp crystals (002) peak (Fan *et al.*, 2015).

In addition, temperature and activation time also have a significant effect on the properties of activated carbon (Lillo-Ródenas *et al.*, 2003). The catalyst/biomass weight ratio and water/biomass ratio also have a significant effect on the crystallinity and SSA of activated carbon (Govindasamy *et al.*, 2022). A more significant amount of water produces in a higher carbonization rate due to the intensification of the hydrolysis reaction (Sermyagina *et al.*, 2015). The high or low water in the HT process affects the pressure during the HT process. The pressure in the HT process affects how quickly volatiles are released, thus forming carbon pores. Pressure affects biomass degradation in the hydrolysis process (Nizamuddin *et al.*, 2017).

* Corresponding author

Email: harsojougm@ugm.ac.id (H. Sabarman)

^aDepartment of Physics, Faculty of Mathematic and Natural Science, Universitas Gadjah Mada, Yogyakarta, 55281, Indonesia

^bResearch Center for Mining Technology, National Research and Innovation Agency, Jl. Ir. Sutami Km. 15 Tanjung Bintang, Lampung Selatan, 35361 Indonesia

However, research on the effect of the ratio of solution to the volume of HT test tube on SSA formed in activated carbon is still limited

The use of different raw materials affects the characteristics of hydrochar. Raw materials and heat treatment of carbon-based materials significantly affect the carbon structure (Li et al., 2019; Schuepfer et al., 2020; Wibawa et al., 2020). Carbon materials, such as charcoal, carbon black, coal, graphite, and carbon fiber have amorphous and crystalline structures with high degrees of crystallinity and gravity. Studying the structure of carbon will help us understand the various heat treatment processes during carbonization (Tyumentsev & Fazlitdinova, 2020). Many studies have been conducted on biomass in their respective regions. Biomass was selected because it is environmentally friendly and abundantly available in nature. The potential of biomass from unused waste needs to be continuously explored and developed to increase added value and support a circular economy and net zero waste.

Various ways for researchers to analyze changes in carbon structure through X-ray diffraction (XRD), HRTEM, and Raman analysis (Saikia *et al.*, 2020; Sharma *et al.*, 2000; Tyumentsev & Fazlitdinova, 2020; Wibawa *et al.*, 2020). Quantitative analysis using XRD is one of the most widely used methods. Through the X-ray diffraction pattern graph, structural carbon parameters such as graphene layer characteristics and the degree of disorder in carbon materials, such as coal and activated carbon, can be observed (Manoj, 2016; Sharma *et al.*, 2000). By studying the content of crystalline and amorphous carbon phases, the main parameters of activated carbon can be determined, such as interlayer spacing and crystallite size. Various treatments in the carbon manufacturing process are carried out to determine the differences in carbon materials and to maintain their regularity.

Physical and chemical activation are often carried out to obtain carbon with high SSA. Chemical activation is usually carried out by soaking using phosphoric acid (H₃PO₄), nitric acid (HNO₃), hydrogen peroxide (H₂O₂), hydrochloric acid (HCl), KOH, and NaOH (Sajjadi *et al.*, 2019). However, activation using chemicals has drawbacks because the liquid waste still contains chemicals. Physical activation of carbon using nitrogen has been widely used. One of the advantages of nitrogen activation is the

subsequent N-doping, which provides advantages to supercapacitor electrode materials (Biniak *et al.*, 1997; Lu *et al.*, 2016). Physical activation using inert gas does not produce hazardous liquid waste, but producing the desired pores in the process is still a challenge. Therefore, combining the HT method and physical activation with N_2 needs to be studied to determine the characteristics of the activated carbon produced.

This research aims to study the effect of HT treatment with various experimental variations on the structure and SSA of activated carbon derived from banana peels. HT parameters include the use of reactant agents H₃PO₄, PEG, deionized water, temperature, and activation time. KOH chemical activator was not used in this study to obtain a more environmentally friendly process. In addition, two carbon precursor treatments without hydrothermal process were also observed. N₂ gas activation was carried out after hydrochar was obtained from the HT process. Banana peels were chosen because of their abundant availability and have added value to banana peel waste from banana chips from micro, small and medium enterprises in Lampung Province. The success of this study spurred the development of activated carbon materials for environmentally friendly supercapacitor electrode applications.

2. Experimental

2.1 Materials and equipment

The materials used in this study were banana peels (Musa paradisiaca L.) obtained from banana chips waste from micro, small, and medium enterprises in Bandar Lampung. Banana peels were washed using plain water then soaked using 1% K_2SO_4 for 24 hours. The banana peels were then rinsed and dried for three days until the maximum water content was 7%. Next, the grinding process is carried out using a planetary ball mill until a size of 0.149~mm is obtained with sample code BP01. Un-milled banana peels are partially wrapped in aluminium foil and then heated in an oven at 200 °C for 6 hours. Then put into a desiccator container, ground, and sieved until it passes a size of 0.149~mm with sample code BP02. BP02 is used as a carbon precursor in the HT process.

Table 1

Specimen –	Hydrothermal Parameter							
	PEG	H ₃ PO ₄ DI Temperature		Holding time				
	(ratio per g)	(ratio pe	r volume)	(°C)	(hrs)			
BP02			Noun	НТ				
BP01			Noun	НТ				
HT1			0.30	200	6			
HT2		0.06	0.70	200	6			
HT3	1		0.70	200	6			
HT4		0.36	0.36	200	6			
HT5	1	0.03	0.30	200	2			
HT6			0.36	200	2			
HT7			0.70	200	2			
HT8	1	0.03	0.30	200	6			
HT9			0.36	200	6			

2.2 Hydrothermal process

Carbon precursor with a fixed weight of 2 grams was mixed with DI and activator agents H_3PO_4 and PEG (2 grams). The materials were mixed and stirred using a magnetic stirrer at a temperature of 60°C for 1 hour. The mixed materials were then put into a Teflon container with a capacity of 35 mL. The HT process was carried out with different compositions at 200°C for 2 hours or 6 hours, which represented fast and long holding times. BP02 that has gone through the HT process is given the HT code according to the composition of the activator agents DI, H_3PO_4 , and PEG, as in Table 1. The biocarbon was then washed using DI, filtered using Whatman 42 filter paper, and dried until it had a max. 7% water content, and then the physical activation process was carried out with N_2 gas flow.

2.3 Nitrogen (N2) activation

 N_2 activation was carried out in a tube furnace operating at a maximum temperature of 900 °C. Some oven-dried biochars (HT1 to HT9) were placed in a cup. The cup was then placed in a tube furnace supplied with N_2 gas. The N_2 gas flow rate was 100 mL/min. The N_2 flow was allowed to run for 30 minutes, and the furnace was turned on. The N_2 activation temperature was 700 °C for 1 hour. Then, it was allowed to cool to room temperature.

2.4 Charactherization

Surface area test (SBET) and porosity were measured using the Brunnauer, Emmett & Teller (BET) method using a TriStar II Plus micropolymer equipped with an analytical balance. Measurements were carried out in liquid nitrogen (temperature 77 K). Before measurement, the biochar was placed in a vacuum container for degassing. SBET observations include mesopores (>2nm) and micropores (<2nm).

Crystallography was analyzed using X-ray diffraction (PANalytical X'pert 3 Powder) with Cu at an angle of 2θ =10-80°. The determination of the background treatment was carried out first by making a graph at coordinates x = 0 and y = 0, so that the surface area was calculated at point 0, as in Figure 3. After the background was removed and set at coordinates (0,0), then smoothing was carried out with the Gaussian fitting process so that the peaks became more symmetrical. Furthermore, the 2θ points and FWHM values were obtained.

The degree of crystallization was calculated based on the ratio of the diffraction intensity of crystal to amorphous, provided that both have the same chemical composition. The relative fraction of crystal and amorphous was calculated at the maximum intensity of the 002 peak. The 002 peak from the X-ray diffraction results was used to determine the structural parameters (d002, Lc) by deconvoluting the asymmetric 002 peak into peaks near 20° and 26°. The degrees of crystallization and amorphous were calculated based on the equations below.

Crystalline carbon (%) =
$$(I_{Crystalline}/I_{Total}) \times 100\%$$
 (1)

Observations using the Bragg and Scherer equations include the degree of crystallinity (X), distance between aromatic layers (d002), height of aromatic layers (Lc), width of aromatic layers (La), and number of aromatic layers (N).

$$X(\%) = \frac{Crystal\ Area}{Crystal\ Area + Amorf\ Area} x\ 100\%$$
 (2)

The distance between the planes can be determined based on the diffraction peak angle. While the crystallite size Lc and La can be calculated using the angle (2 theta) and full width at half maximum (FWHM). The grain size Lc and La along the coordinates c and a are calculated from the reflections (002) and (100) using the Scherer equation, while the observation of d002 uses the Bragg equation. The grain size describes the number of layers in the stack.

$$L_a = \frac{1.84 \,\lambda}{B_a \cos \varphi_a} \tag{3}$$

$$L_c = \frac{0.89 \,\lambda}{B_c \cos \varphi_c} \tag{4}$$

$$d_{002} = \frac{\lambda}{2\sin\theta} \tag{5}$$

Where λ is the wavelength of radiation, B_a and B_c are FWHM (100) and (002) in radians, respectively, φ_a and φ_c are appropriate scattering angles.

Number of aromatic lamellae can be determined by the equation (6).

$$N = \frac{L_{002} + D_{002}}{D_{002}} \tag{6}$$

SEM morphological analysis was performed using a Field Emission Scanning Electron Microscope (FESEM) type Thermo Scientific Quattro S with a magnification of 20,000X. The sample after the nitrogen activation process without preparation treatment was in the form of a final powder. The differences between each treatment were compared to determine the effect of each treatment on the pores formed in activated carbon.

3. Results and Discussion

3.1 Surface area (m²/g) BET

Activated carbon from banana peels in this study had SSA ranging from 2.96 to 476.91 m²/g, as shown in Table 2. Meanwhile, activated carbon without HT treatment and direct physical activation using N2 gas had low SSA with values of 2.96 m²/g and 9.54 m²/g, respectively. The N₂ activation process without HT produced a relatively lower SBET compared to the pyrolysis carbonization process (Y. Zhang et al., 2019). The surface area of activated carbon produced from the HT process has a higher value, namely 53.41 m²/g to 476.91 m²/g. This value is in line with previous studies that carried out biomass activation using HT. In previous studies that carried out activation at the same temperature and holding time, 200 °C for 6 hours, biomass-based hydrocarbons produced SSA of 7.1 to 10.7 m²/g respectively (Fang et al., 2015). Increasing the temperature from 200 to 250 °C at the same holding time did not increase the SSA value, so the selection of a temperature of 200 °C in this study was appropriate.

Researches conducted using the same material, namely banana peel, but using H₃PO₄ solution as a chemical activator produced an SSA of 28.80-45.27 m²/g (Zhou, Chen, Feng, *et al.*, 2017). H₃PO₄, as an activation agent, will interact with carbon precursors during the soaking process by breaking the aryl ether bonds. H₃PO₄ is a breaker of aryl ether and lignin bond chains and hydrolyzes glycosidic bonds in cellulose and hemicellulose through dehydration and condensation processes (Oginni *et al.*, 2019). As explained in previous studies, activation using H₃PO₄ solution can increase activated carbon SBET. Biochar from kenaf fiber has an SBET of 13.68 m²/g and increases to 299.02 m²/g (Shamsuddin *et al.*, 2016). In line with other studies, using

Table 2Specific surface area and pore volume of activated carbon obtained from BET

Specimen code	Specific Surface Area (m2/g)	Smicro (m²/g)	/g) Smicro/SBET		
BP02	9.54	3.72	39%		
BP01	2.95	0.58	20%		
HT1	53.41	42.29	79%		
HT2	176.15	134.29	76%		
HT3	411.50	50.96	12%		
HT4	471.97	80.47	17%		
HT5	476.90	235.45	49%		
HT6	204.00	162.03	79%		
HT7	222.52	192.50	87%		
HT8	470.24	71.37	15%		
HT9	428.20	31.36	7%		

 H_3PO_4 can increase the SBET of wood biochar by up to 1.7 times (Nitnithiphrut *et al.*, 2017).

The use of H₃PO₄ for banana peel activation in this study resulted in a much higher SSA compared to previous studies. This study showed an 18.4-fold increase in carbon precursors wi th H₃PO₄ activation. This increase continued with the addition of the H₃PO₄ volume ratio concentration to 0.36 with an SBET of 471.99 m²/g. The addition of the H₃PO₄/DI ratio of 0.06/0.70 resulted in an SSA of 176.15 m²/g, increasing with the increase in the H₃PO₄/DI volume ratio of 0.36/0.70, resulting in an SBET of 471.99 m²/g. These results are much greater than previous studies using 50% H₃PO₄, only producing an SSA of 28.80 m²/g (Zhou, Chen, Feng, et al., 2017). The difference in the process in the two studies lies in the duration of removal and further activation using N2 gas flow. This difference in the process shows that physical activation using inert gas affects the formation of SSA. Argon (Ar) and Nitrogen (N2) are inert gases that are often used. The difference in inert gas activation produces different SBET even with the same raw materials. Previous experiments using Ar inert gas at a temperature of 900 °C for 1 hour produced a high SBET of 194 m²/g (Y. Zhang et al., 2016). In addition to different inert gases, pre-activation processes, and physical activation temperatures also have an effect. Previous studies have conducted physical activation of N_2 from carbon precursors derived from banana peel pyrolysis. Preheating at 300 °C for 0.5 hour and carbonization at 800 °C for 3 hours with nitrogen flow produced SBET of 201.33 m²/g (Yan et al., 2018). The pretreatment process and physical activation parameters of N2 also affect the SSA value of activated carbon. However, the hydrothermal process before N₂ activation also shows its effect on the SSA value of activated carbon.

Increasing the solution volume ratio from 0.3 to 0.36 resulted in SBET of 53.41 and 470.25 m²/g. The addition of the solution volume ratio has an impact on increasing the pressure in the hydrothermal process. Increasing the pressure in the hydrothermal process will have an impact on higher levels of dehydration and aromatization. However, this phenomenon occurs at a certain point, only sometimes increasing hydrothermal pressure will produce high SSA of activated carbon (Yu et al., 2022). Pressure and holding time in the hydrothermal process must be considered to obtain maximum carbon SSA. In samples with a DI volume ratio of 0.7 and a holding time of 2 hours, it produced 222.53 m²/g, lower than the ratio of 0.36 with a longer holding time. At the same volume ratio, namely 0.36 with a holding time of 2 and 6 hours, the SSA produced 204.0 and 428.21 m²/g, respectively. This increase indicates a directly proportional effect between the holding time and the SSA of activated carbon.

The use of PEG6000 with a ratio of 1/1 to carbon precursor at a DI volume ratio of 0.7 increased the SSA value from 222.53 to $411.50 \, \text{m}^2/\text{g}$. PEG can encourage the formation of new pores so that the surface area of carbon increases actively. PEG functions as a surfactant that can reduce surface and interfacial tension, thus encouraging the formation of more pores in biochar. According to Tu et~al.~(2019), PEG can affect the distribution of hydrothermal products because it is hydrophilic or lipophilic, which can create a layer to increase the hydrothermal carbonization of biomass (Tu et~al.~(2019)).

Comparison of specific surface area (BET) of activated carbon made from banana peel can be seen in Table 3. It is clear that an activation by hydrothermal method can occur in environmental conditions compared to pyrolysis. Activator agents, such as using KOH, are often added to the hydrothermal process to increase SSA. However, the importance of an environmentally friendly activation process by reducing the use of KOH. In addition to being dangerous, KOH also provides an expensive process because the ratio used is still too high. The carbonization process by pyrolysis method followed by activation using an activator agent provides very high SSA. In general, the SSA obtained from the pyrolysis process is higher than hydrothermal.

The percentage of Smicro/SBET ratio is significant because micropores play an important role in the adsorption behavior of activated carbon. A high percentage of Smicro/SBET may indicate the active role of the activator in removing tar that clogs the pores of biochar (Oginni $\it et al., 2019$). The highest pore surface area (m²/g) was obtained when the DI volume ratio increased to 0.7. Increasing the solution volume in the autoclave reaction vessel increased the pressure

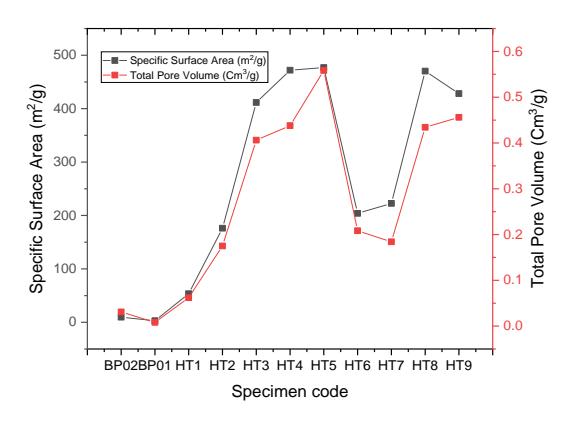


Fig. 1 Total pore volume (cm³/g) of activated carbon

Table 3Comparison of specific surface area (BET) of banana peel-based activated carbon

Carbonization method	Activator	Temperature	SSA (BET) (m2/g)	Referensi
	DI Water	200°C – 6hrs	428.21	
Hydrothermal & N_2	H_3PO_4	200°C – 6hrs	471.98	this research
	PEG6000 + H ₃ PO ₄	200°C – 6hrs	476.91	
Hydrothermal	Water + Ethanol	200°C -24hrs	294.60	(Nguyen et al., 2022)
Hydrothermal	H_3PO_4	240°C - 2hrs	4.68	(Bai et al., 2024)
Hydrothermal	H_3PO_4	230°C - 2hrs	31.65	(Zhou, Chen, Xi, <i>et al.</i> , 2017)
Hydrothermal	КОН	180°C - 3hrs	243.40	
Hydrothermal	КОН	200°C - 3hrs	154.60	(Goel et al., 2024)
Hydrothermal	КОН	220°C - 3hrs	71.72	
Pyrolisis & N_2	K_2CO_3	850°C - 2hrs	2159	(Wang <i>et al.</i> , 2018)
Pyrolisis & N ₂	MgO	850°C - 2hrs	1691.00	(Wang et al., 2016)
Pyrolisis & N ₂		800°C - 3 hrs	201.33	(Yan <i>et al.</i> , 2018)
Pyrolisis & N ₂		800°C - 3 hrs	1330.01	(1 dil et at., 2016)
Pyrolisis	КОН	900°C	1362.00	(Fasakin <i>et al.</i> , 2018)
Pyrolisis	H ₃ PO ₄	850°C	218.33	(Gautam <i>et al.</i> , 2024)

Table 4Analysis of variance for HT parameter on SBET & Summary for Transformed Response

Analysis of variance for HT parameter on SBET								Summary for Transformed Response		
Source	DF	Seq SS	Contribution	Adj SS	Adj MS	F-Value	P-Value	S	R-sq	R-sq (adj)
PEG	1	182.417	31.65%	14.408	14.408	2.01	0.251	2.67671	96.27	87.57
H_3PO_4	3	114.157	19.81%	36.076	12.0253	1.68	0.34			
DI	3	258.304	44.82%	258.304	86.1012	12.02	0.035			
Error	3	21.494	3.73%	21.494	7.1648					
Total	10	576.372	100.00%							

experienced by the carbon precursor during the hydrothermal process. High pressure promotes the formation of increased pore surface area.

Based on the test results shown in Figure 1, the SSA of activated carbon is directly proportional to the total pore volume. The total pore volume (cm³/g) is also low when the SSA is low. Conversely, when the SSA is high, the total pore volume (cm³/g) is also high. The lowest total pore volume (cm³/g) was obtained for activated carbon without HT treatment.

Analysis of variance (ANOVA) was conducted to determine the effect of activating agents on the hydrothermal process because in physical activation with a constant N2 gas flow rate against temperature and holding time, these process parameters are ignored. The ANOVA results are shown in Table 4. PEG, H₃PO₄ and DI play a role in the SSA value of activated carbon. The maximum error (α) in ANOVA was set at 5%, meaning that the P value should not be more than 0.05 to be able to reject the null hypothesis (H0). The ANOVA results show the contribution of each activating agent, PEG, H₃PO₄, and DI. In sequence, the contributions of PEG, H₃PO₄, and DI are 31.65%, 19.81%, and 44.82%. DI provides the widest distribution of activated carbon pores. DI also has a P value that is still within the tolerance limit, less than $\alpha = 5\%$, indicating that DI has a significant effect on the SSA value of activated carbon. While other activating agents, PEG and H₃PO₄, do not have a significant effect. The

error obtained from the experimental results was 3.73% or had a data distribution confidence level of R-sq of 96.27%, still below the value of $\alpha=5\%$.

3.2 X-ray diffraction

The XRD method was used to observe the crystal structure of activated carbon. The graph produced from the XRD test is shown in Figure 2. The XRD graph shows two different peak characteristics at an angle of 20 around 26° and 43°. These two peaks are at hkl (002) and (100). No peaks were observed in the raw material compared to other specimens. Sample BP02 and Sample BP01 are activated carbon materials without HT process treatment. Banana peel powder was carbonized directly using a tube furnace at a temperature of 700 °C for 1 hour, with N₂ gas flowing at a flow rate of 100 mL/min. Without HT treatment, activated carbon forms a highly amorphous structure and an irregular surface. Based on the amorphous fraction in the specimen without HT process, it reached 94.75%. The absence of significant peaks during the activation process indicates a high amorphous fraction, unlike the specimen that went through the HT process, where a more dominant peak structure appeared to be formed. The HT process involves heating reactants in a closed vessel at a certain pressure to form a material with a better crystal structure (Adame-Pereira et al.,

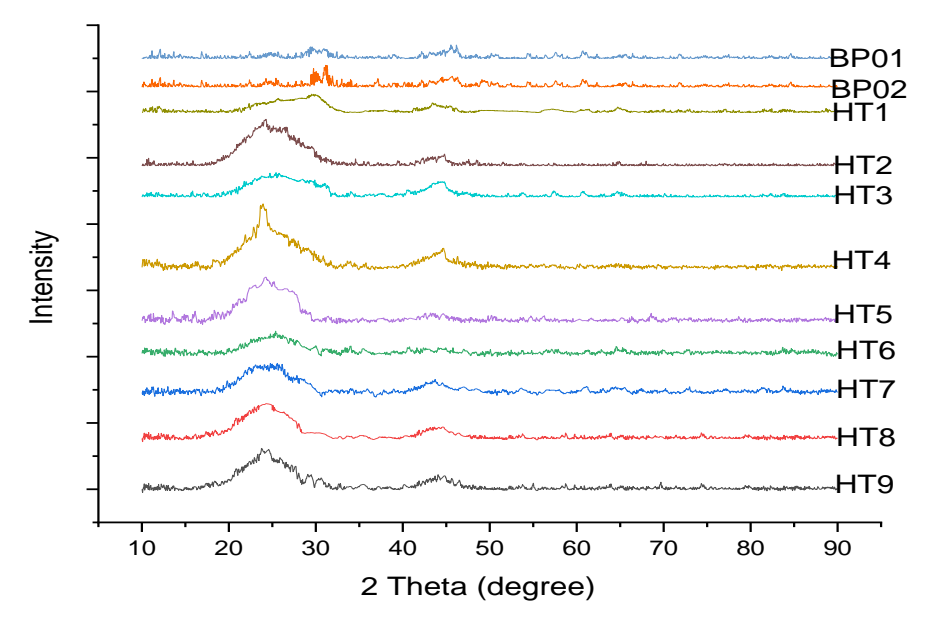


Fig. 2 X-ray diffraction patterns of activated carbon for raw material, 2hrs, and 6 hrs

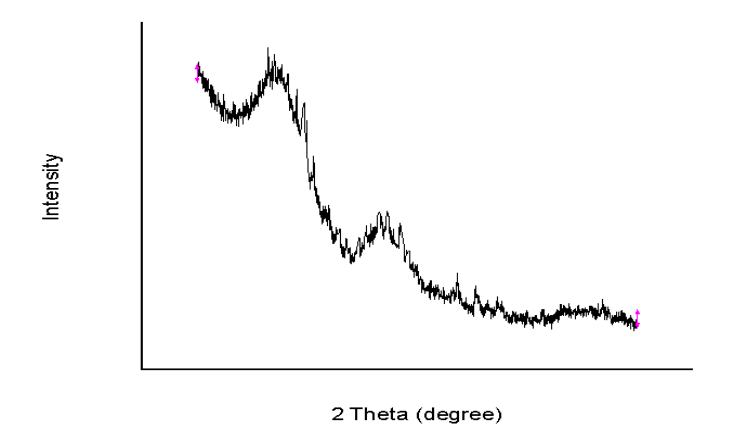


Fig. 3 Fitting of XRD patterns of activated carbon using Gaussian peaks

2023). The closed-container process allows for controlled environmental conditions to be more stable and a better crystal structure to be obtained. The HT process can also increase the adsorption capacity of activated carbon compared to traditional pyrolysis processes by increasing the porosity and surface area of activated carbon (Zhao *et al.*, 2009).

Based on the graph produced from X-ray diffraction, there is a peak change around 2θ:26°. Figure 3 shows several treatments of activated carbon forming asymmetric peaks. This asymmetric structure indicates that activated carbon does not have well-defined and regular graphite crystals. The regularity of the peak in the 002 region shows the same structure as the graphite structure (Zhao et al., 2009). The diffraction angle (2 θ) of the 002 peak of graphite crystals is known to be 26.56°. However, some samples experience a shift in the 002 peak. The greater distance between the planes in this activated carbon indicates the presence of heteroatoms, irregular structures, and material defects in the activated carbon (Lee et al., 2021). This asymmetric peak also affects the crystallite size, as indicated by the increase in the FWHM value. The FWHM value is inversely proportional to the crystallite size of activated carbon (La and Lc) (Lee et al., 2021).

The structural parameters of activated carbon obtained from XRD are shown in Table 5. The errors that occur are still high, ranging from 3.4% to 13.6% for specimens HT5 and HT6. The inaccuracy of this data iteration is caused by the irregular distribution of values on the X-ray diffraction graph. This irregularity indicates defects in the specimen (Lee *et al.*, 2021). The number of aromatic lamellae (N) in the range of 2.3 to 3.7 indicates an important structural component of the carbon material. HT treatment and the addition of active materials in the HT process increase the number of aromatic lamellae (N). These aromatic lamellae are a planar arrangement of hexagonal carbon rings. The number of lamellae indicates the level of gravity and structural properties of the activated carbon material.

There is no observable peak in the raw material compared to other specimens. Sample BP02 and Sample BP01 are activated carbon materials without HT process treatment. Banana peel powder was directly carbonized using a tube furnace at a temperature of 700 °C for 1 hour, with N_2 gas flowing at a 100 mL/min flow rate. Without HT treatment, activated carbon formed a highly amorphous structure and an irregular surface. In research conducted by Yan *et al.* (2018), the

Table 5Structural parameter of activated carbon obtained from XRD

Specimen	Crystalline	Amorphous	d002	Lc (Å)	d10l	La (Å)	N
code	Fraction (%)	Fraction (%)					
BP02	15.42	84.58	3.47	8.1	1.99	27.8	2.6
BP01	5.25	94.75	3.66	9.65	1.99	65.66	2.3
HT1	46.49	53.51	3.62	12.94	2.07	32.37	3.5
HT2	41.08	58.92	3.53	11.00	2.06	53.66	2.7
HT3	54.49	45.51	3.66	9.33	2.08	35.82	2.5
HT4	59.96	40.04	3.48	8.65	2.03	25.86	2.4
HT5	67.08	32.92	3.67	13.74	2.05	34.05	3.7
HT6	78.74	21.26	3.21	41.1	2.06	53.66	3.1
HT7	68.04	31.96	3.36	12.37	2.06	57.16	3.6
HT8	55.77	44.23	3.44	10.78	2.06	43.33	3.2
HT9	61.87	38.13	3.62	12.78	2.06	45.88	3.5

peak angles occurred at positions 2θ : ~23° (002) and ~44° (100). According to Yan and Co, the 2θ position corresponds to amorphous carbon with a disordered internal structure (Yan *et al.*, 2018). Conversely, smaller crystallites indicate a more amorphous or irregular structure. Carbon parameters for Lc values are 6.43 to 7.35 Å. La is at a peak of 4.12 Å. Based on La and Lc, the d002 value was 3.21 to 3.67. According to Lee *et al.* (2021), graphitizable activated carbon was at d002 between 3.36–3.44 Å, with Lc and La values depending on the degree of graphitization (Lee *et al.*, 2021). The specimen with the H_3PO_4 activation agent is closest to the graphite crystal at 3.35.

The carbon maturity index indicating the degree of gravity development and structure of activated carbon is shown in Figure 4. The carbon maturity index is directly proportional to the layer height but inversely proportional to the distance between layers. In contrast, the aromaticity of activated carbon is directly proportional to the layer height and distance. The carbon maturity index is closely related to the aromatic lamella. The existence of aromatic structures contributes to the mechanical properties and thermal stability of activated carbon. The properties of activated carbon are fundamental when used in high temperature applications or environments with high chemical content.

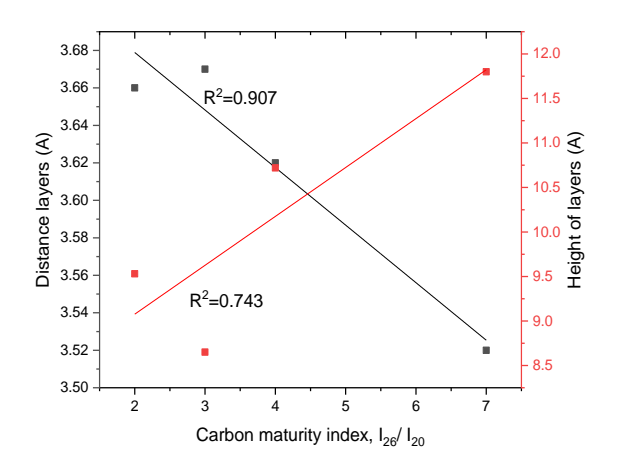
3.3 FESEM of activated carbon

The morphology of activated carbon observed by FESEM with a magnification of 20,000X is shown in Figure 5. The

morphology of activated carbon with N_2 gas flow without HT treatment appears uneven and porous as seen in Figure 5 (a). The surface is uneven and rough due to the presence of protrusions and grooves on the surface of the activated carbon. The cavities are formed due to the role of nitrogen gas as a gentle oxidizer to remove volatile components from the carbon precursor, thus only damaging the surface. The physical activation process using nitrogen can open pores in the inner carbon layer, so that the surface area formed still needs to be larger.

The two-stage carbon activation process showed complex and interconnected pores, as shown in Figure 5 (b). The carbon surface has been mostly degraded into small grains with smaller pore surfaces. The two-stage activation included activation by the HT method using a reaction tube/DI volume ratio of 0.36 at a temperature of 200 °C for 2 hours, followed by physical activation with nitrogen gas flow. This two-stage activation process is better than the one-stage activation on specimens BP01 and BP02.

There is a significant difference compared to the activation process using only nitrogen gas flow or HT activation using DI as its activator. H_3PO_4 produces particles that tend to be spherical, as shown in Figure 5 (c). The exact spherical structure also occurred in previous studies using H_3PO_4 as an activating agent on rose twig charcoal material. The spherical characteristics of activated carbon are very beneficial when used in supercapacitor electrode applications (Si *et al.*, 2019). Unlike other activations, this activation tends to have an



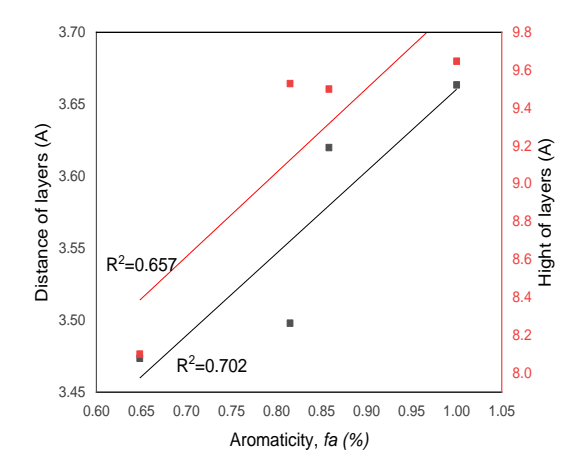


Fig. 4 The relation of carbon maturity index and aromaticity of activated carbon

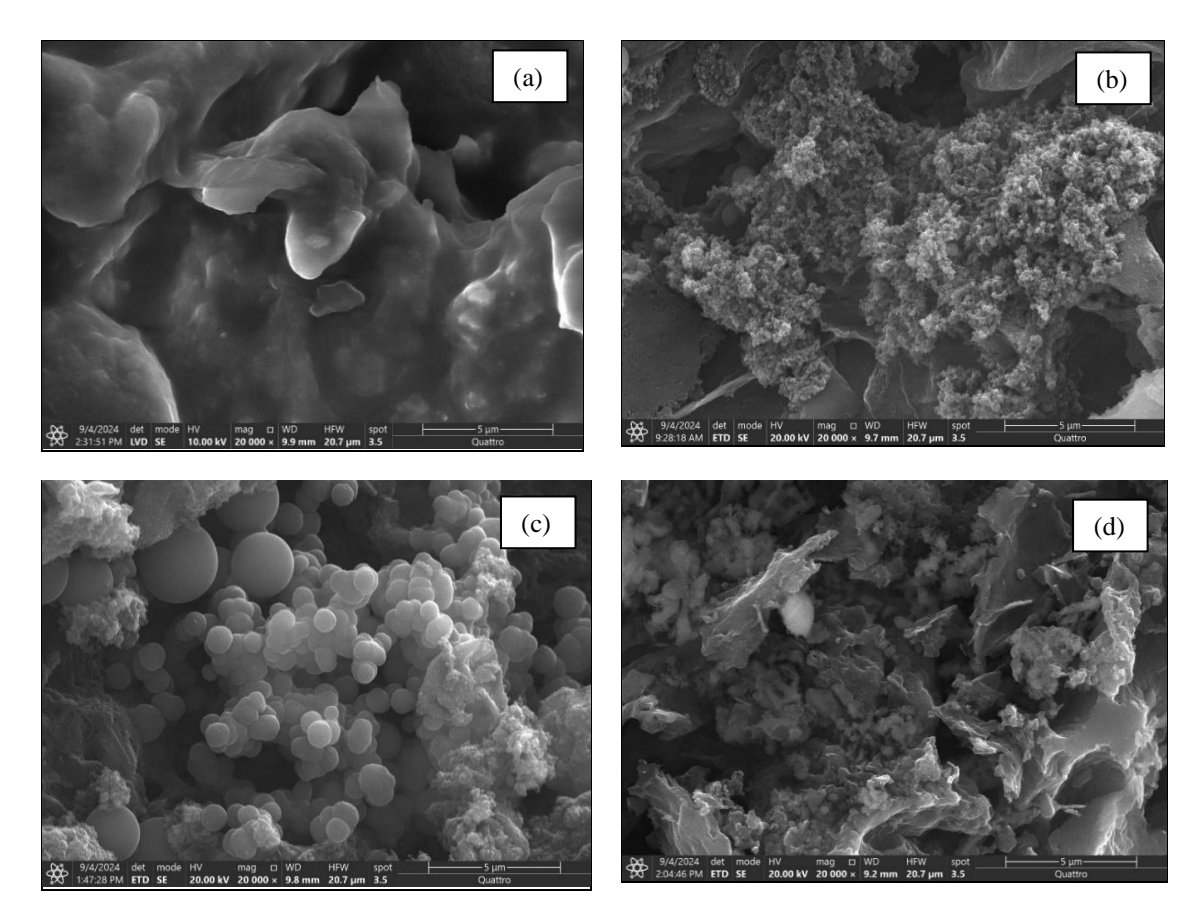


Fig. 5 The morphology of activated carbon is taken from FESEM images at 20,000X magnification; a). One-stage activation process using nitrogen gas flow (N_2) without hydrothermal process; b). The two-stage activation process, using deionized water with a ratio to the volume of the test tube of 0.36 at a temperature of 200 °C for 6 hours; c). Two-stage activation process with N_3PO_4 activator agent; d). Two-stage activation process with PEG 6000 activator agent.

irregular structure. The spherical particles in activation using H_3PO_4 tend to be uniform, although clumping is still visible, so that the cavity has not formed optimally. Phosphate ions (PO_4^{3-}) act as templates that bind and form carbon structures. A low DI/test tube volume ratio of 0.06 provides sufficient H_3PO_4 concentration to form a porous carbon structure. At a higher DI/test tube volume ratio, these spherical pores become fewer due to the decreasing H_3PO_4 concentration.

Activation with the addition of PEG 6000 shows the carbon surface resembles a thin sheet that overlaps each other, as shown in Figure 5 (d). The rough and degraded surface shape forms a different angle from activation using $H_{\rm 3}PO_{\rm 4}$, which is round. PEG 6000 molecules are used as soft templates to form pore structures on carbon and then removed during heating, leaving a porous structure. Activation using PEG 6000 produces more layers with cavities on the carbon surface. The combination of PEG 6000 and $H_{\rm 3}PO_{\rm 4}$ provides more pore space, thereby increasing the surface area of carbon.

4. Conclusion

Carbon activation from banana peel waste from production has been carried out using one-stage and two-stage activation processes. One-stage activation was carried out using N_2 gas flow, while two-stage activation was carried out using the hydrothermal method followed by physical activation of N_2 gas flow.

Hydrothermal activation increased the specific surface area (SBET) of activated carbon from banana peel waste. The ratio of deionized water volume to total volume had a significant effect and contributed 44.82%. High pressure due to increased DI volume and longer holding time promoted the formation of increased surface area. At the same time, other activating agents, PEG and H_3PO_4 , contributed 31.65% and 19.81%. HT post-treatment with N_2 gas flow activation helped to form pores and increase the surface area of SBET activated carbon.

Hydrothermal treatment produces two characteristic peaks that differ at 20 angles of about 26° and 43°. These two peaks are located at hkl (002) and (100). These peaks indicate the degree of gravity of activated carbon. This peak does not occur in activated carbon without HT process and is characterized by a high degree of amorphous, reaching 94.75%. The shift of the 002 peak of crystalline graphite 26.56°, characterized by graph broadening and asymmetry, indicates the irregularity of the carbon structure. The surface morphology of activated carbon is greatly influenced by the activation process and the activator agent used. The two-stage activation process produces a porous surface structure compared to one-stage activation. The activator agent H₃PO₄ gives the effect of forming regular spherical grains, while the use of PEG6000 forms a porous layer. The combination of activator agents has an impact on better surface area.

Studying the effect of environmentally friendly HT process by utilizing biomass waste on the specific surface area and carbon structure is expected to be used in wide applications such as EDLC supercapacitor electrode materials, battery cathodes, and adsorption materials.

Acknowledgments

The authors acknowledge the facilities, scientific and technical support from Advanced Characterization Laboratories Lampung, National Research and Innovation Agency through E-Layanan Sains, Badan Riset dan Inovasi Nasional. Research funding is mostly by DIPA ORNM - BRIN.

Author Contributions: All authors contributed equally, have read and agreed to the published version of the manuscript.

Funding: The author(s) received no financial support for publication of this article.

Conflicts of Interest: The authors declare no conflict of interest.

References

- Adame-Pereira, M., Durán-Valle, C. J., & Fernández-González, C. (2023). Hydrothermal Carbon Coating of an Activated Carbon—A New Adsorbent. *Molecules*, 28(12). https://doi.org/10.3390/molecules28124769
- Bai, T., Yao, Y., Zhao, J., Tian, L., & Zhang, L. (2024). Adsorption Performance and Mechanism of H3PO4-Modified Banana Peel Hydrothermal Carbon on Pb(II). Separations, 11(1). https://doi.org/10.3390/separations11010017
- Biniak, S., Szymański, G., Siedlewski, J., & Światkoski, A. (1997). The characterization of activated carbons with oxygen and nitrogen surface groups. *Carbon*, *35*(12), 1799–1810. https://doi.org/10.1016/S0008-6223(97)00096-1
- Fan, L. Q., Liu, G. J., Zhang, C. Y., Wu, J. H., & Wei, Y. L. (2015). Facile one-step hydrothermal preparation of molybdenum disulfide/carbon composite for use in supercapacitor. *International Journal of Hydrogen Energy*, 40(32), 10150–10157. https://doi.org/10.1016/j.ijhydene.2015.06.061
- Fang, J., Gao, B., Chen, J., & Zimmerman, A. R. (2015). Hydrochars derived from plant biomass under various conditions: Characterization and potential applications and impacts. Chemical Engineering Journal, 267, 253–259. https://doi.org/10.1016/j.cej.2015.01.026
- Fasakin, O., Dangbegnon, J. K., Momodu, D. Y., Madito, M. J., Oyedotun, K. O., Eleruja, M. A., & Manyala, N. (2018). Synthesis and characterization of porous carbon derived from activated banana peels with hierarchical porosity for improved electrochemical performance. *Electrochimica Acta*, 262, 187–196. https://doi.org/10.1016/j.electacta.2018.01.028
- Gautam, M., Patodia, T., Gupta, V., Sachdev, K., & Himmat S. Kushwaha. (2024). Synthesis of high surface area activated carbon from banana peels biomass for zinc-ion hybrid supercapacitor. *Journal of Energy Storage*, 102 Part A(114088). https://doi.org/https://doi.org/10.1016/j.est.2024.114088
- Goel, C., Mohan, S., Dinesha, P., & Rosen, M. A. (2024). CO2 adsorption by KOH-activated hydrochar derived from banana peel waste. *Chemical Papers*, 78(6), 3845–3856. https://doi.org/10.1007/s11696-024-03355-z
- Govindasamy, G., Sharma, R., & Subramanian, S. (2022). Catalytic Hydrothermal Liquefaction of Sugarcane Bagasse: Effect of Crystallization Time of Fe-MCM-41 and Process Parameters. *Bulletin of Chemical Reaction Engineering and Catalysis*, 17(4), 768–777. https://doi.org/10.9767/BCREC.17.4.15781.768-777
- Lee, S. M., Lee, S. H., & Roh, J. S. (2021). Analysis of activation process of carbon black based on structural parameters obtained by XRD analysis. *Crystals*, *11*(2), 1–11. https://doi.org/10.3390/cryst11020153
- Lestari, D. I., Yuliansyah, A. T., & Budiman, A. (2022). Adsorption

- studies of KOH-modified hydrochar derived from sugarcane bagasse for dye removal: Kinetic, isotherm, and thermodynamic study. *Communications in Science and Technology*, 7(1), 15–22. https://doi.org/10.21924/cst.7.1.2022.669
- Li, X., Gu, M., Zhang, F., Min, Q., & Chen, L. (2019). Effects of raw materials on the structures of three dimensional graphene/amorphous carbon composites derived from biomass resources. *Research on Chemical Intermediates*, 45(3), 1131–1145. https://doi.org/10.1007/s11164-018-3669-5
- Lillo-Ródenas, M. A., Cazorla-Amorós, D., & Linares-Solano, A. (2003).
 Understanding chemical reactions between carbons and NaOH and KOH: An insight into the chemical activation mechanism.
 Carbon, 41(2), 267–275. https://doi.org/10.1016/S0008-6223(02)00279-8
- Lin, Y., Xu, H., Gao, Y., & Zhang, X. (2023). Preparation and characterization of hydrochar-derived activated carbon from glucose by hydrothermal carbonization. *Biomass Conversion and Biorefinery*, 13(5), 3785–3796. https://doi.org/10.1007/s13399-021-01407-y
- Lu, Z., Lu, J., Li, X., & Shao, G. (2016). Effect of MgO addition on sinterability, crystallization kinetics, and flexural strength of glass-ceramics from waste materials. *Ceramics International*, 42(2), 3452-3459. https://doi.org/10.1016/j.ceramint.2015.10.142
- MacDermid-Watts, K., Pradhan, R., & Dutta, A. (2021). Catalytic hydrothermal carbonization treatment of biomass for enhanced activated carbon: a review. *Waste and Biomass* https://doi.org/10.1007/s12649-020-01134-x
- Manoj, B. (2016). A comprehensive analysis of various structural parameters of Indian coals with the aid of advanced analytical tools. *International Journal of Coal Science and Technology*, 3(2), 123–132. https://doi.org/10.1007/s40789-016-0134-1
- Nguyen, T. N., Le, P. A., & Phung, V. B. T. (2022). Facile green synthesis of carbon quantum dots and biomass-derived activated carbon from banana peels: synthesis and investigation. *Biomass Conversion and Biorefinery*, 12(7), 2407–2416. https://doi.org/10.1007/s13399-020-00839-2
- Nitnithiphrut, P., Thabuot, M., & Seithtanabutara, V. (2017). Fabrication of Composite Supercapacitor Containing Para Wood-derived Activated Carbon and TiO2. *Energy Procedia*, 138, 116–121. https://doi.org/10.1016/j.egypro.2017.10.074
- Nizamuddin, S., Baloch, H. A., Griffin, G. J., Mubarak, N. M., Bhutto, A. W., Abro, R., Mazari, S. A., & Ali, B. S. (2017). An overview of effect of process parameters on hydrothermal carbonization of biomass. *Renewable and Sustainable Energy Reviews*, 73(December 2016), 1289–1299. https://doi.org/10.1016/j.rser.2016.12.122
- Nonchana, T., & Pianthong, K. (2020). Bio-oil synthesis from cassava pulp via hydrothermal liquefaction: Effects of catalysts and operating conditions. *International Journal of Renewable Energy Development*, 9(3), 329–337. https://doi.org/10.14710/ijred.9.3.329-337
- Oginni, O., Singh, K., Oporto, G., Dawson-Andoh, B., McDonald, L., & Sabolsky, E. (2019). Effect of one-step and two-step H3PO4 activation on activated carbon characteristics. *Bioresource Technology Reports*, 8(July), 100307. https://doi.org/10.1016/j.biteb.2019.100307
- Saikia, B. K., Benoy, S. M., Bora, M., Tamuly, J., Pandey, M., & ... (2020).

 A brief review on supercapacitor energy storage devices and utilization of natural carbon resources as their electrode materials.

 Fuel.

 https://www.sciencedirect.com/science/article/pii/S0016236 120317920
- Sajjadi, B., Chen, W. Y., & Egiebor, N. O. (2019). A comprehensive review on physical activation of biochar for energy and environmental applications. *Reviews in Chemical Engineering*, 35(6), 735–776. https://doi.org/10.1515/revce-2017-0113
- Schuepfer, D. B., Badaczewski, F., Guerra-Castro, J. M., Hofmann, D. M., Heiliger, C., Smarsly, B., & Klar, P. J. (2020). Assessing the structural properties of graphitic and non-graphitic carbons by Raman spectroscopy. *Carbon*, *161*, 359–372. https://doi.org/10.1016/j.carbon.2019.12.094
- Sermyagina, E., Saari, J., Kaikko, J., & Vakkilainen, E. (2015). Hydrothermal carbonization of coniferous biomass: Effect of process parameters on mass and energy yields. *Journal of*

- Analytical and Applied Pyrolysis, 113, 551–556. https://doi.org/10.1016/j.jaap.2015.03.012
- Shamsuddin, M. S., Yusoff, N. R. N., & Sulaiman, M. A. (2016). Synthesis and Characterization of Activated Carbon Produced from Kenaf Core Fiber Using H3PO4 Activation. *Procedia Chemistry*, *19*, 558–565. https://doi.org/10.1016/j.proche.2016.03.053
- Sharma, A., Kyotani, T., & Tomita, A. (2000). Comparison of structural parameters of PF carbon from XRD and HRTEM techniques. *Carbon*, *38*(14), 1977–1984. https://doi.org/10.1016/S0008-6223(00)00045-2
- Si, H., Wang, B., Chen, H., Li, Y., Zhang, X., Liang, X., Sun, L., Yang, S., & Hou, D. (2019). Activated Carbon Prepared from Rose Branch using H3PO4- hydrothermal Carbonization and Activation and its Apllication for Supercapacitors. *International Journal of Electrochemical Science*, 14(8), 7899–7910. https://doi.org/10.20964/2019.08.49
- Tu, R., Sun, Y., Wu, Y., Fan, X., Wang, J., Shen, X., He, Z., Jiang, E., & Xu, X. (2019). Effect of surfactant on hydrothermal carbonization of coconut shell. *Bioresource Technology*, 284(February), 214–221. https://doi.org/10.1016/j.biortech.2019.03.120
- Tyumentsev, V. A., & Fazlitdinova, A. G. (2020). Investigation of Changes in the Fine Structure of Graphitizing Carbon Materials during Heat Treatment by X-Ray Diffraction Analysis. *Journal of Materials Science and Chemical Engineering*, 08(10), 11–20. https://doi.org/10.4236/msce.2020.810002
- Wang, Q., Zhou, M., Zhang, Y., Liu, M., Xiong, W., & Liu, S. (2018). Large surface area porous carbon materials synthesized by direct carbonization of banana peel and citrate salts for use as highperformance supercapacitors. *Journal of Materials Science: Materials in Electronics*, 29(5), 4294–4300. https://doi.org/10.1007/s10854-017-8376-2
- Wibawa, P. J., Nur, M., Asy'ari, M., & Nur, H. (2020). SEM, XRD and FTIR analyses of both ultrasonic and heat generated activated carbon black microstructures. *Heliyon*, 6(3), e03546. https://doi.org/10.1016/j.heliyon.2020.e03546
- Yan, Y., Wei, Y., Li, Q., Shi, M., Zhao, C., Chen, L., Fan, C., Yang, R., & Xu, Y. (2018). Activated porous carbon materials with ultrahigh specific surface area derived from banana peels for high-

- performance lithium–sulfur batteries. *Journal of Materials Science: Materials in Electronics*, *29*(13), 11325–11335. https://doi.org/10.1007/s10854-018-9220-z
- Yu, S., Zhao, P., Yang, X., Li, Q., Mohamed, B. A., Saad, J. M., Zhang, Y., & Zhou, H. (2022). Low-temperature hydrothermal carbonization of pectin enabled by high pressure. *Journal of Analytical and Applied Pyrolysis*, 166(July), 105627. https://doi.org/10.1016/j.jaap.2022.105627
- Zhang, B., Heidari, M., Regmi, B., Salaudeen, S., Arku, P., Thimmannagari, M., & Dutta, A. (2018). Hydrothermal carbonization of fruit wastes: A promising technique for generating hydrochar. *Energies*, 11(8), 1–14. https://doi.org/10.3390/en11082022
- Zhang, Y., Gao, Z., Song, N., & Li, X. (2016). High-performance supercapacitors and batteries derived from activated bananapeel with porous structures. *Electrochimica Acta*, *222*, 1257–1266. https://doi.org/10.1016/j.electacta.2016.11.099
- Zhang, Y., Jiang, Q., Xie, W., Wang, Y., & Kang, J. (2019). Effects of temperature, time and acidity of hydrothermal carbonization on the hydrochar properties and nitrogen recovery from corn stover. *Biomass and Bioenergy*, 122(May 2018), 175–182. https://doi.org/10.1016/j.biombioe.2019.01.035
- Zhao, J., Yang, L., Li, F., Yu, R., & Jin, C. (2009). Structural evolution in the graphitization process of activated carbon by high-pressure sintering. *Carbon*, 47(3), 744–751. https://doi.org/10.1016/j.carbon.2008.11.006
- Zhou, N., Chen, H., Feng, Q., Yao, D., Chen, H., Wang, H., Zhou, Z., Li, H., Tian, Y., & Lu, X. (2017). Effect of phosphoric acid on the surface properties and Pb (II) adsorption mechanisms of hydrochars prepared from fresh banana peels. *Journal of Cleaner Production*, 165, 221–230. https://doi.org/10.1016/j.jclepro.2017.07.111
- Zhou, N., Chen, H., Xi, J., Yao, D., Zhou, Z., Tian, Y., & Lu, X. (2017). Biochars with excellent Pb(II) adsorption property produced from fresh and dehydrated banana peels via hydrothermal carbonization. *Bioresource Technology*, 232(Ii), 204–210. https://doi.org/10.1016/j.biortech.2017.01.074



© 2025. The Author(s). This article is an open access article distributed under the terms and conditions of the Creative Commons Attribution-ShareAlike 4.0 (CC BY-SA) International License (http://creativecommons.org/licenses/by-sa/4.0/)